PERGAMON

International Journal of Impact Engineering 26 (2001) 93–104

INTERNATIONAL JOURNAL OF IMPACT ENGINEERING

www.elsevier.com/locate/ijimpeng

BALLISTIC LIMIT EQUATIONS FOR SPACECRAFT SHIELDING

ERIC L. CHRISTIANSEN* and JUSTIN H. KERR*

*NASA Johnson Space Center, Mail Code SN3, Houston, TX 77058

ABSTRACT—This paper provides equations describing the ballistic performance capability of meteoroid/orbital debris (M/OD) shield systems employed on the International Space Station (ISS). Hypervelocity impact (HVI) tests and analysis were used in developing the semi-empirical ballistic limit equations (BLE). A description of each type of shield system, HVI tests and analysis performed to assess shield performance, and ballistic limit equations that define the protection capability of the shield are given. Methods to improve the performance of spacecraft shielding are also discussed.

Keywords: shielding, meteoroid/orbital debris protection, ballistic limit equations

NOTATION

C	Speed of sound in target (km/s)
d	projectile diameter (cm)
d_c	critical projectile diameter causing shield failure (cm)
ρ	density (g/cm^3)
H	Brinnell hardness of target (BHN)
m	areal density (g/cm^2)
M	projectile mass (g)
P	penetration depth (cm)
S	overall spacing between outer bumper and rear wall (cm)
σ	rear wall yield stress (ksi) (Note: 1ksi = 1,000 lb$_f$/in^2 = 6.895 MPa)
σ'	normalized rear wall yield stress (unitless)
t	thickness (cm)
θ	impact angle measured from normal to surface (deg)
V	projectile velocity (km/s)
V_n	normal component of impact velocity (km/s)

Subscripts:

b	all bumpers
p	projectile
t	target
w	rear wall
1..3	individual bumpers, layers or spacings

INTRODUCTION

The International Space Station (ISS) represents one of the largest and most ambitious space vehicle design and on-orbit construction programs ever executed. Because of its large size (>12,000 m^2 surface area) and long lifetime (15 years), the ISS will be exposed to a large number

0734-743X/01/$ - see front matter
PII: S0734-743X(01)00070-7

of hypervelocity impacts (HVI) from meteoroids and orbital debris. For example, over 30,000 meteoroid/orbital debris (M/OD) impact craters greater than 0.3mm diameter were counted on the exterior of the Long Duration Exposure Facility (LDEF) [1]. The exposure of ISS to M/OD impacts is an estimated 250 times greater than LDEF in terms of area-time exposed to the M/OD flux. To insure crew safety, ISS crew modules and external critical components will be better protected from meteoroid/orbital debris impact than previously flown spacecraft.

A variety of shield types are used to protect ISS critical items from M/OD (Fig.1). These include Whipple, Nextel™/Kevlar™ Stuffed Whipple, and Multi-Shock shields [2]. Whipple shields are basically 2 layer shields, an outer "bumper" and an inner "rear wall", with a gap or "standoff" between the two. A Stuffed Whipple (SW) shield has a blanket of Nextel™/Kevlar™ between the bumper and rear wall. Multi-Shock (MS) shields have multiple bumpers followed by one or more rear walls.

This paper provides data and ballistic limit equations (BLEs) characterizing the performance of shields used on portions of the ISS Node 1, U.S. Laboratory and Airlock Modules, and Service Module (Fig. 2). These shields vary in terms of their mass per unit area ("areal density"), standoff (or deployed volume) and protection capability. The BLEs have been developed from hypervelocity impact tests and analysis. NASA and ISS hardware providers use the BLEs in computer tools such as the BUMPER code to assess the probability of no penetration (PNP) for ISS critical item shielding [2]. In addition, the BLEs are useful as a benchmark to measure the protection performance versus mass and standoff of future shield developments. The BLEs presented in this paper are subject to updates based on additional HVI testing and analysis.

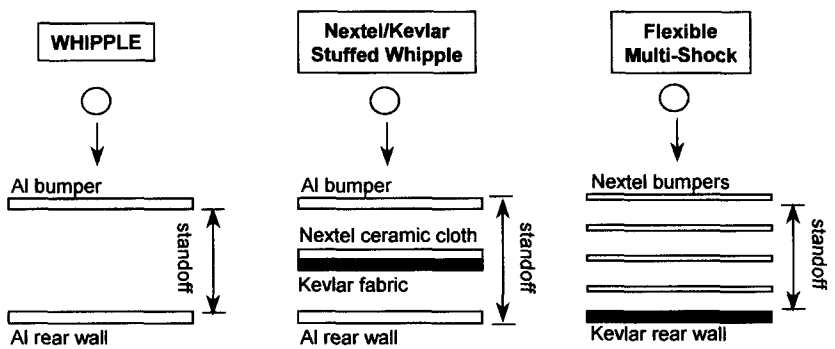

Fig. 1. M/OD Shield Types

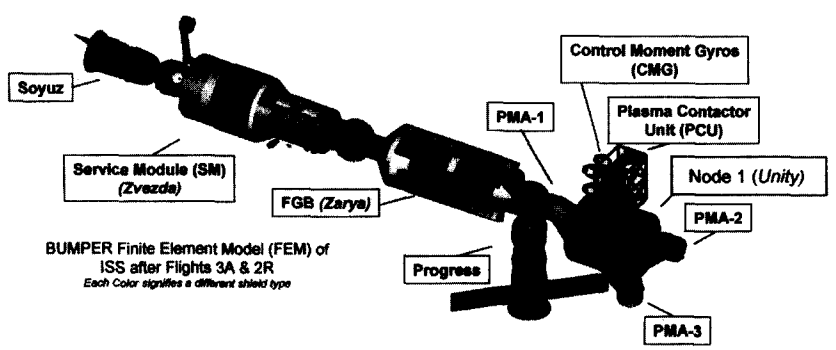

Fig. 2. ISS after assembly Flight 3A (solar arrays removed for clarity)

™ Nextel is a trademark of 3M Corporation, Kevlar is a trademark of DuPont Company Inc.

HVI TEST FACILITIES

Light-gas gun (LGG) launchers at the NASA Ames Research Center (ARC) and NASA Johnson Space Center (JSC) were used to perform hypervelocity impact (HVI) tests on ISS shielding [3,4]. LGG launcher bore diameters ranged from 12.7mm to 25.4mm. This paper summarizes results from over 200 LGG tests that were performed to characterize the performance of selected ISS shielding. The LGG tests varied from 2 to 7.5 km/s. In addition, HVI tests have been performed on prototype ISS shields at velocities up to 11.5 km/s using the inhibited shaped charge launcher (ISCL) at Southwest Research Institute (SwRI) and the hypervelocity launcher (HVL) at Sandia National Laboratories (SNL).

BALLISTIC LIMIT EQUATIONS

Semi-empirical equations for Whipple and Multi-Shock shields were previously developed to fit high-velocity (≥7 km/s), normal-angle impact conditions [5-7]. Early versions of semi-empirical ballistic limit equations for shielding used on ISS were described previously [8].

For the BLEs presented in this paper, the particle is assumed to be spherical and homogenous. The BLEs describe the particle diameter, d_c, causing failure of the shield as a function of projectile impact conditions (i.e., impact speed or velocity, impact angle, and impactor density). Particles that impact with diameters above the "critical" diameter defined by the BLEs will fail the shield.

Failure Criteria. "Failure" of the shield is defined as either complete penetration (i.e., perforation) or detached spall from the back of the shield's rear wall. In the case of ISS crew modules (for example, Node 1, U.S. Lab, and SM), the pressure shell is the rear wall of the shield. Fig. 3 shows a schematic of typical failure and no-failure modes after Cour-Palais and Dahl [9]. Generally, Whipple shields exhibit detached spall failure combined with or instead of perforation failure. Detached spall failures do not generally occur with Nextel/Kevlar Stuffed Whipple or Multi-Shock shields.

Damage Class C3: Detached spall ***Damage Class C4: Perforation***

Fig. 3. Typical rear wall failure modes (Cour-Palais and Dahl, 1993)

Impact Physics. A typical BLE for a Whipple shield is illustrated in Fig. 4 compared to a monolithic, single layer of same mass as the combined Whipple shield's bumper and rear wall. Protection capabilities are defined for three penetration regimes based on normal component velocity for an aluminum impact on a Whipple shield. Important shield physical and material properties are included in the ballistic limit equations.

At low impact velocities, below 3 km/s, impact shock pressures are low and the projectile remains essentially intact after bumper impact. A deformed but substantially intact projectile then impacts the shield's rear wall. The projectile is more damaging as velocity increases in the low velocity regime. At velocities above 3 km/s, the projectile fragments to a larger extent upon impact on the bumper and will begin to melt above V_n of 5.5 km/s for aluminum on aluminum impacts. Damage to the rear wall decreases as the projectile is fragmented and partially melted, thus the protection capability of the shield (in terms of the critical particle size on the failure threshold of the shield) increases with velocity in the intermediate velocity regime. At high velocities (V_n > 7 km/s), the debris cloud impacting the rear wall will contain various fractions of solid, liquid, and vapor components of the projectile and bumper depending on impact conditions (bumper thickness, density, projectile diameter, density, shape, impact obliquity, etc.). A simple

analytical relationship forms the basis of scaling to velocities beyond 8 km/s, the upper limit of two-stage LGG database. As such, the critical particle diameter decreases with increasing velocity in the high velocity regime.

Generalized BLEs for major categories of shielding, for example Whipple and Stuffed Whipple shields, have been developed. The generalized BLEs are suitable for predicting ballistic performance for a wide range of shield parameters. Specific BLEs, applicable for individual shield configurations only, have been developed to be more accurate for the applicable shield configuration only.

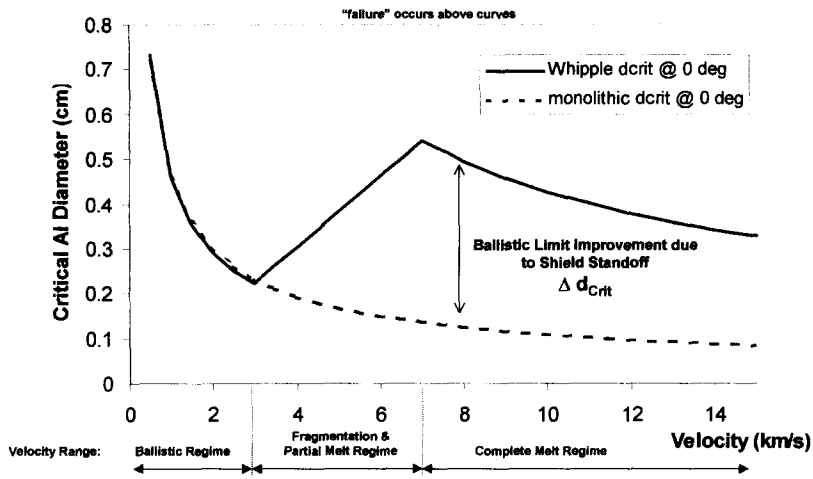

Fig. 4. Illustration of Ballistic Limits for Monolithic and Whipple Shield (equal mass).
Failure criterion is shield threshold perforation or detached spall from rear wall. Monolithic is 0.44cm thick Al 6061T6. Whipple is 0.12cm thick Al 6061T6 bumper followed at 10cm by 0.32cm Al 6061T6 rear wall.

WHIPPLE SHIELDS

Generalized Whipple Shield BLEs in Equations 1-3 have been modified to account for a wider range of shield parameters than the original equations previously provided [8]. Figure 5 illustrates the ability of the generalized equations to predict the ballistic limit particle size for about 200 tests in the JSC Whipple shield database. This database varied over a large range of impact and target parameters. The projectiles in these tests varied from 0.02cm diameter to 1.9cm diameter, impact velocities from 2 km/s to over 8 km/s, and impact angles from normal (0°) to 75°. Most of the tests used aluminum spherical impactors although copper, steel and nylon projectiles are represented in the database. The Whipple shields varied in this database from bumper thickness to projectile diameter (t_b/d) ratios of less than 0.05 to over 1.0, and S/d varied from 3 to over 140. The targets in these tests did not contain multilayer insulation (MLI) although additional tests have been performed to quantify the effect of MLI. Figure 5 provides the ratio of test projectile diameter to the predicted particle size using Eqn. (1-3) on the ballistic limit of the shields as a function of normal component velocity of the tests. Shield failure is predicted when the diameter ratio is larger than 1.0, and no failure below the ratio=1.0 line. For this database, there are very few actual test failures when no-failure is predicted. Over 90% of the database was predicted accurately from a safety standpoint (failures predicted accurately), whereas the same figure of merit was 77% using the previous equations [8]. It should be noted that either set of generalized equations provides a prediction that is reasonably close to the actual shield ballistic limit. However, major changes in these equations from previous versions [8] that make them more applicable to a wider range of target conditions include the incorporation of bumper thickness dependence in the high velocity equation. In addition, the equations are applicable for all two-wall shield systems with or without MLI present between bumper & rear

wall (0.05-0.06 g/cm^2). When MLI is present, the critical particle size is improved (increased) in the intermediate velocity regime because the MLI acts to slow/defeat fragments that lead to detached spall and/or perforation of the rear wall if the MLI is not present.

High-Velocity: when $V \geq V_H/(\cos\theta)$,

$$d_c = k_h \rho_p^{-1/3} (V\cos\theta)^{-2/3} \rho_b^{-1/9} S^{1/2} (t_w \rho_w)^{2/3} \sigma'_h{}^{1/3} + \Delta_{MLI} \quad (1)$$

Where V_H = 7km/s, k_h = 1.35 unless $t_b/(t_w^{2/3} S^{1/2}) < 0.126$, then $k_h = 7.451\ t_b/(t_w^{2/3} S^{1/3}) + 0.411$. The units on k_h are {cm$^{1/2}$ km$^{2/3}$ g$^{-2/9}$ s$^{-2/3}$}. Also, normalized yield stress (unitless) $\sigma'_h = (\sigma/70\text{ksi})$. The effect of MLI on the critical particle size is given by Δ_{MLI} (cm). MLI is more effective in raising critical particle size the closer it is to the rear wall (S_{MLI} is the distance from the bumper to the MLI). The delta critical particle size due to MLI is found from the following equation where m_{MLI} is the areal density of the MLI (g/cm^2) and k_{MLI}=1.4cm^2:

$$\Delta_{MLI} = k_{MLI}\, m_{MLI} (S_{MLI}/S)^{1/2}$$

Intermediate-Velocity: when $V_L/(\cos\theta)^{1.5} < V < V_H/(\cos\theta)$,

$$d_c = [k_{hi}\ \rho_p^{-1/3} \rho_b^{-1/9} S^{1/2} (t_w \rho_w)^{2/3} \sigma'_h{}^{1/3} + \Delta_{MLI}\ ]\ [V - V_L(\cos\theta)^{-1.5}] / [V_H(\cos\theta)^{-1} - V_L(\cos\theta)^{-1.5}]$$
$$+\ k_{li} (t_w \sigma'_L{}^{0.5} + C_L t_b \rho_b)\ \rho_p^{-0.5} (\cos\theta)^{(-5/6)} [V_H(\cos\theta)^{-1} - V] / [V_H(\cos\theta)^{-1} - V_L(\cos\theta)^{-1.5}] \quad (2)$$

Where V_L = 3km/s with no MLI present and V_L = 2km/s when MLI is present, k_{hi} {cm$^{1/2}$ g$^{-2/9}$} = $V_H^{-2/3} k_h$, k_{li} {g$^{0.5}$ cm$^{-3/2}$} = $V_L^{-2/3} k_l$, C_L=0.37 cm^3/g, and normalized yield stress (unitless) $\sigma'_L = (\sigma$ / 40ksi)

Low-Velocity: when $V \leq V_L/(\cos\theta)^{1.5}$,

$$d_c = k_l (t_w \sigma'_L{}^{0.5} + C_L t_b \rho_b)\ (\cos\theta)^{-11/6} \rho_p^{-0.5} V^{-2/3} \quad (3)$$

Where k_l = 1.9 {g$^{0.5}$ km$^{2/3}$ cm$^{-3/2}$ s$^{-2/3}$}. There is an impact angle cutoff for oblique impacts above 65° to account for the increased damage to the rear wall from bumper fragments at extreme impact angles, i.e., d_c (θ>65°) = d_c (θ=65°).

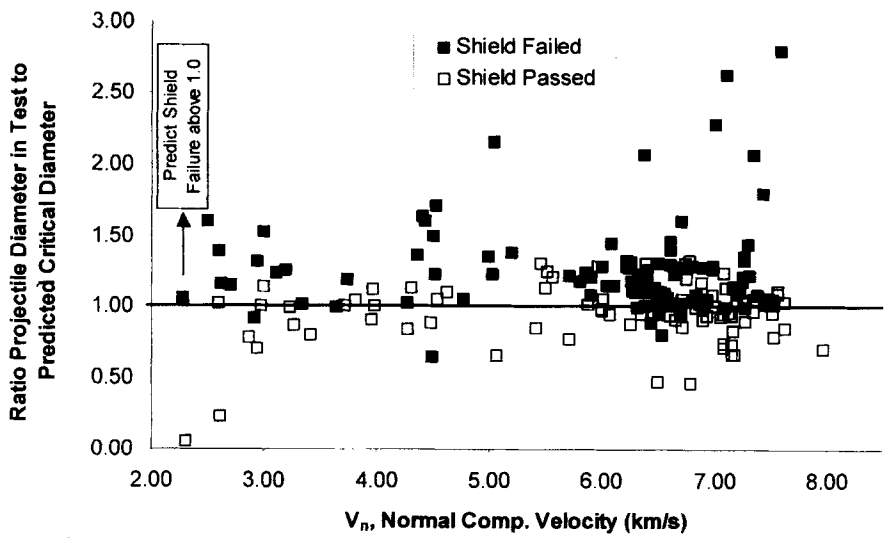

Fig. 5. Predictions from Eqn.1-3 for 200 different Whipple Shield HVI tests

Specific Whipple Shield BLEs for ISS. Whipple shields are used to protect parts of the U.S. Laboratory Common Module (CM), "Unity" Node 1 module, and Service Module (SM) (Fig.2). Cylinder sections of CM and Node have shorter standoffs (~10.7cm) while endcone (EC) sections have larger standoffs (~22cm). These shields include 42 layer multi-layer insulation (MLI) thermal blankets typically 4cm behind the bumper, with an average areal density of 0.054 g/cm^2. Whipple shielding also protects portions of the "Zvezda" Service Module (SM) on ISS. Specific BLEs have been defined for the SM working compartment small diameter cylinder section (zone 6, 19.7m^2, 13% of total SM area) and SM working compartment large diameter cylinder section (zones 10 & 11, 38.1 m^2, 25% of total SM area) based on results of HVI test data. These areas of SM have a 0.10cm thick aluminum AMG-6 outer bumper, a thermal blanket (areal density = 0.06 g/cm2) mounted on rear wall, a 0.16cm (zone 6) to 0.2cm (zone 10&11) thick aluminum AMG-6 rear wall, and 5cm standoff (gap between bumper & rear wall). Whipple shield BLEs have been updated to reflect the presence of MLI blankets. Equations 4-6 provide the critical particle, d_c (cm), at the detached spall or perforation failure limit of the rear wall of the specific ISS shields given in Table 1. Predicted ballistic limits and HVI test data are given in Fig. 6-9 for the US Lab and Node Cylinder and Lab endcone shields. Figures 10 and 11 show the location of SM shields and BLEs for the SM small diameter cylinder shields. There is an impact angle cutoff constraint for oblique impacts above 65°, i.e., d_c (θ>65°) = d_c (θ=65°). Table 1 provides coefficients for the equations.

High-Velocity: when $V \geq V_H/(\cos\theta)^{xh}$,

$$d_c = K_H \rho_p^{-1/3} (V \cos\theta)^{-2/3} \tag{4}$$

Intermediate-Velocity: when $V_L/(\cos\theta)^{xl} < V < V_H/(\cos\theta)^{xh}$,

$$d_c = K_{hi} \rho_p^{-1/3} (\cos\theta)^{(-2/3 + xh * 2/3)} [V - V_L(\cos\theta)^{-xl}] / [V_H(\cos\theta)^{-xh} - V_L(\cos\theta)^{-xl}]$$
$$+ K_{li} \rho_p^{-0.5} (\cos\theta)^{(-4/3 + el + xl * 2/3)} [V_H(\cos\theta)^{-xh} - V] / [V_H(\cos\theta)^{-xh} - V_L(\cos\theta)^{-xl}] \tag{5}$$

Low-Velocity: when $V \leq V_L/(\cos\theta)^{xl}$,

$$d_c = K_L (\cos\theta)^{(-4/3 + el)} \rho_p^{-0.5} V^{-2/3} \tag{6}$$

Table 1. Whipple shield BLE coefficients and variables

	CM cylinder	CM EC tb=0.2cm	Node fwd cylinder	Node aft cylinder	Node EC tb=0.13cm	Node EC tb=0.2cm	SM cylinder Zone 6	SM cylinder Zone 10&11
Mat'l t_b	Al6061T6	Al6061T6	Al6061T6	Al6061T6	Al6061T6	Al6061T6	AMG6	AMG6
Mat'l t_w	Al2219T87	Al2219T87	Al2219T87	Al2219T87	Al2219T87	Al2219T87	AMG6	AMG6
t_b (cm)	0.2	0.2	0.13	0.13	0.13	0.2	0.1	0.1
S (cm)	10.7	22.2	10.7	10.9	22.2	22.1	5	5
t_w (cm)	0.48	0.48	0.64	0.41	0.58	0.58	0.16	0.2
K_H ($g^{1/3}$ $km^{2/3}$ $s^{-2/3}$)	7.6	9.64	5.5	6.6	7.16	9.1	1.876	2.076
K_N ($g^{1/3}$)	2.077	2.634	1.503	1.770	1.957	2.487	0.513	0.567
K_{li} ($g^{1/2}$ $cm^{-1/2}$)	1.145	1.145	0.760	0.839	0.819	0.706	0.289	0.319
K_L ($g^{1/2}$ $cm^{-1/2}$ $km^{2/3}$ $s^{-2/3}$)	1.5	1.5	1.4	1.1	1.3	1.3	0.602	0.663
V_H (km/s)	7	7	7	7.2	7	7	7	7
V_L (km/s)	1.5	1.5	2.5	1.5	2	2	3	3
x_h	1	1	1	1	1	1	1	1
x_l	1.9	1.9	1.9	1.5	1	1	1	1
e_l	θ<60°: -1/3 θ>=60°: -2/3	-0.5	θ<60°: -1 θ>=60°: -2/3	θ<60°: -1/3 θ>=60°: -2/3	θ<60°: -1/6 θ>=60°: -2/3	-0.5	-1/3	-1/3

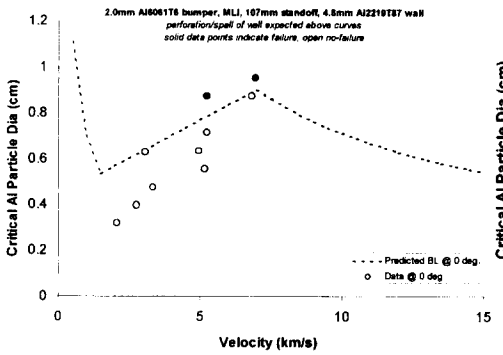

Fig. 6. US Lab Cylinder Whipple Shield Ballistic Limits @ 0° impact angle

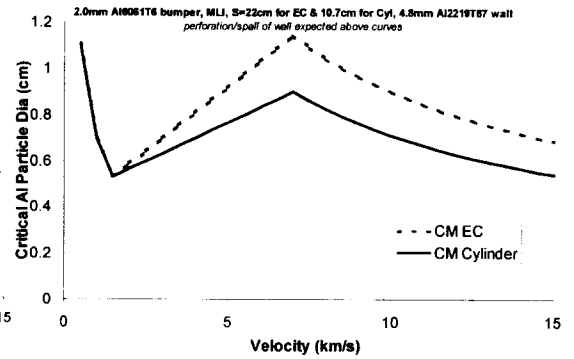

Fig. 7. US Lab Cylinder (S=10.7cm) and Endcone (S=22cm) Ballistic Limits @ 0°

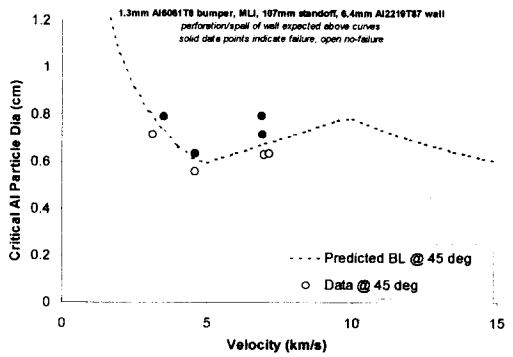

Fig. 8. Node 1 Forward Cylinder Whipple Shield Ballistic Limits @ 45° impact angle

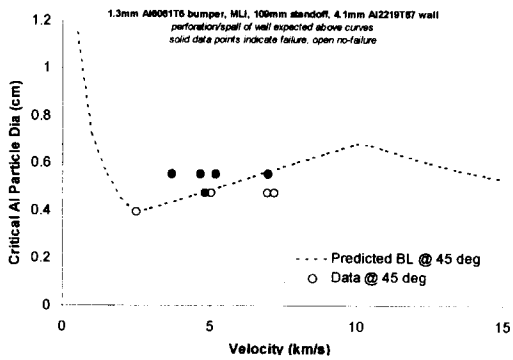

Fig. 9. Node 1 Aft Cylinder Whipple Shield Ballistic Limits @ 45° impact angle

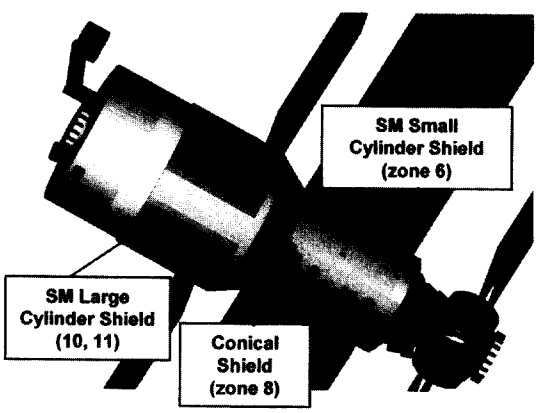

Fig. 10. Service Module (SM) Shield Locations

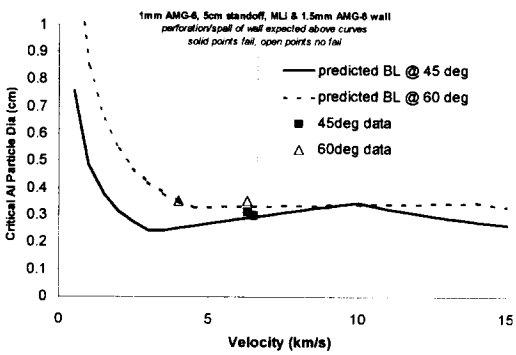

Fig. 11. SM Zone 6 Whipple Shield Ballistic Limits at 45° and 60° impact angle

Nextel™/Kevlar™ STUFFED WHIPPLE SHIELDS

Nextel™/Kevlar™ "Stuffed" Whipple (SW) shields protect sections of ISS that are exposed to the highest concentration of orbital debris and meteoroid impacts. For instance, the baseline shielding for high M/OD flux areas of the ISS U.S. Lab and Airlock modules will incorporate a blanket between the outer aluminum bumper and inner pressure wall that combines two materials: Nextel™ ceramic fabric and Kevlar™ high strength fabric. NASA developed this shield to improve spacecraft protection from meteoroid/orbital debris (M/OD) impact over that offered by conventional 2-sheet Whipple shields. Figure 1 illustrates a typical SW configuration. A major advantage of the ceramic cloth is that it generates higher shock pressures and greater disruption of an impacting particle than an equivalent weight aluminum bumper. High-strength Kevlar™ cloth follows the ceramic cloth. Because it has a much higher strength to weight ratio than aluminum, Kevlar™ is more effective at slowing any remaining projectile fragments and decreasing the expansion rate of the debris cloud before it subsequently impacts the rearwall of the shield. Other high-strength fabrics such as Spectra™ have also demonstrated good performance in HVI tests [10-11].

A general set of equations that can also be used to predict SW ballistic limits are given in Eqns.7-9. These equations are subject to change based on additional HVI tests. For instance, HVI test data indicates that the current ballistic limit equations for the Stuffed Whipple shields are in some cases conservative (i.e., under predict critical spherical particle size) at velocities >10 km/s from the inhibited shaped charge and HVL launchers. More near-term experimental and hydrocode work is planned to improve the assessment on effects of non-spherical projectile shapes and projectile velocity.

High-Velocity: when $V \geq 6.5/(\cos\theta)^{3/4}$,

$$d_c = K_{H\text{-}SW} (t_w \rho_w)^{1/3} \rho_p^{-1/3} V^{-1/3} (\cos\theta)^{-0.5} S^{2/3} \sigma'^{1/6} \quad (7)$$

Where the normalized rear wall yield strength, $\sigma' = \sigma/40$, and the coefficient, $K_{H\text{-}SW} = 0.6$ km$^{1/3}$/s$^{1/3}$.

Intermediate-Velocity: when $2.6/(\cos\theta)^{0.5} < V < 6.5/(\cos\theta)^{3/4}$,

$$d_c = K_{Hi\text{-}SW} (t_w \rho_w)^{1/3} \rho_p^{-1/3} (\cos\theta)^{-0.25} S^{2/3} \sigma'^{1/6} [(V - 2.6/(\cos\theta)^{0.5})/(6.5/(\cos\theta)^{3/4} - 2.6/(\cos\theta)^{0.5})]$$
$$+ K_{Li\text{-}SW} \rho_p^{-1/2} [t_w \sigma'^{0.5} + C_L m_b] (\cos\theta)^{-1} [[(6.5/(\cos\theta)^{3/4} - V)/(6.5/(\cos\theta)^{3/4} - 2.6/(\cos\theta)^{0.5})] \quad (8)$$

Where $K_{Hi\text{-}SW} = 0.321$, C_L=0.37 cm^3/g and $K_{Li\text{-}SW} = 1.243$ g$^{0.5}$/cm$^{3/2}$.

Low-Velocity: when $V \leq 2.6/(\cos\theta)^{0.5}$,

$$d_c = K_{L\text{-}SW} V^{-2/3} (\cos\theta)^{-4/3} \rho_p^{-1/2} [t_w \sigma'^{0.5} + C_L m_b] \quad (9)$$

Where $K_{L\text{-}SW} = 2.35$ g$^{0.5}$ km$^{2/3}$ cm$^{-3/2}$ s$^{-2/3}$, C_L=0.37 cm^3/g, and the total bumper areal density is the sum of the areal densities of the outer bumper, Nextel, Kevlar and MLI: $m_b = m_1 + m_{Nextel} + m_{Kevlar} + m_{MLI}$.

MULTI-SHOCK SHIELDS

Multi-shock shielding using all flexible materials (fabrics and foams) is under consideration for protecting inflatable modules from meteoroid/debris impact, as well as other hardware on ISS [2, 12]. These shields consisting of Nextel™ ceramic fabric bumpers and Kevlar™ high strength rear wall. Previously described ballistic limit equations [12] have been updated based on further evaluation of shielding capability including HVI testing at NASA White Sands Test Facility and the University of Dayton Research Institute.

Design equations for a flexible multi-shock shield for V_n > 6.4 km/s are given below. Equation 10 gives the areal density of all 4 ceramic bumpers.

$$m_b = 0.185\, d\, \rho_p \tag{10}$$

The areal density of the Kevlar rear wall is estimated from Equation 11, where K = 29 s/km.

$$m_w = K\, M\, V_n / S^2 \tag{11}$$

Ballistic limit equations for flexible multi-shock shields are given in Equations 12-14. These will be updated based on results of on-going HVI tests and analyses. Figure 12 provides a comparison of protection capabilities of equal-weight multi-shock and Whipple shielding. Multi-shock shields are more efficient than Whipple shields at breaking up projectiles, converting projectile kinetic energy into internal energy of projectile fragments, decreasing the velocity of the debris cloud impacting the rear wall. These factors contribute to make multi-shock shielding more effective than Whipple shields for the weight.

High-Velocity: when $V \geq 6.4/(\cos\theta)^{0.25}$,

$$d_c = K_{H\text{-}MS}\, m_w^{1/3}\, S^{2/3}\, \rho_p^{-1/3}\, V^{-1/3}\, (\cos\theta)^{-1/3} \tag{12}$$

Where $K_{H\text{-}MS} = 0.41\ km^{1/3}\, s^{-1/3}$.

Intermediate-Velocity: when $2.4/(\cos\theta)^{0.5} < V < 6.4/(\cos\theta)^{0.25}$,

$$d_c = K_{Hi\text{-}SW}\, m_w^{1/3}\, S^{2/3}\, \rho_p^{-1/3}\, (\cos\theta)^{-1/4}\, [(V - 2.4/(\cos\theta)^{0.5})/\, (6.4/(\cos\theta)^{0.25} - 2.4/(\cos\theta)^{0.5})]$$
$$+\ K_{Li\text{-}SW}\, \rho_p^{-1/2}\, [C_W\, m_w + C_L\, m_b]\, (\cos\theta)^{-1}\, [[(6.4/(\cos\theta)^{0.25} - V)/(6.4/(\cos\theta)^{0.25} - 2.4/(\cos\theta)^{0.5})] \tag{13}$$

Where $K_{Hi\text{-}MS} = 0.221$, $K_{Li\text{-}MS} = 1.506\ g^{1/2}\, cm^{-3/2}$, $C_W = 0.5\ cm^3/g$, $C_L = 0.37\ cm^3/g$.

Low-Velocity: when $V \leq 2.4/(\cos\theta)^{0.5}$,

$$d_c = K_L\, V^{-2/3}\, (\cos\theta)^{-4/3}\, \rho_p^{-1/2}\, [C_W\, m_w + C_L\, m_b] \tag{14}$$

Where $K_L = 2.7\ g^{1/2}\, km^{2/3}\, cm^{-3/2}\, s^{-2/3}$, $C_W = 0.5\ cm^3/g$, $C_L = 0.37\ cm^3/g$.

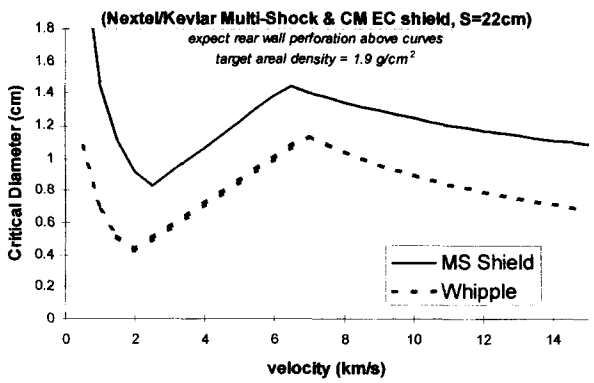

Fig. 12. Equal Weight Whipple and Multi-Shock Shield Ballistic Limits (0° impact) for 22cm Standoff (1.9 g/cm^2 shield mass per unit area)

COMPARISON OF ISS SHIELDS

A comparison of ISS shielding in terms of overall areal density and particle stopping capability in terms of d_c (for 7 km/s, normal impact, aluminum spherical projectiles) is given in Table 2.

Table 2. ISS Shield Summary

Shield	Type	Total Mass per unit area (kg/m^2)	standoff (cm)	d_c (cm) @ 7 km/s, 0°
CM cylinder	Whipple	19.7	10.7	0.9
Node Fwd cylinder	Whipple	22.1	10.7	0.79
Node Aft cylinder	Whipple	15.6	10.9	0.68
CM endcone	Whipple	19.7	22.3	1.14
Node endcone	Whipple	22.7	22.1	1.23
SM small dia cylinder	Whipple	8.9	5	0.35
Soyuz OM Baseline	Whipple	6.3	1.5	0.19
Soyuz OM Option 2	Whipple	7.5	1.5	0.29
CM cylinder	Stuffed Whipple	27.6	10.7	1.34

DISCUSSION OF SHIELDING IMPROVEMENT AND WEIGHT REDUCTION TECHNIQUES

Typically, a spacecraft shield designer will expend efforts improving the spacecraft's M/OD shielding and reducing shielding weight. An iterative shielding analysis/option evaluation process is often employed in the process [2]. The main idea is to identify the "risk drivers" and/or "weight drivers" in a particular spacecraft's protection system, and concentrate on reducing risks or optimizing shielding in these areas. NASA utilizes BUMPER code M/OD risk assessments as an important part of this process. The BLEs given in this paper are programmed into BUMPER and used to assess penetration risks. From the BLEs, several simple methods can be employed to improve shielding effectiveness and/or reduce shielding weight.

1. Increase standoff. Figure 7 shows the effect of standoff increase for the CM cylinder and endcone shielding. Critical particle size increase at 7 km/s, normal impact is 25% larger with the standoff increase from 10.7cm to 22cm.
2. Insure best-possible projectile breakup by using proper bumper thickness and materials. An old rule-of-thumb is that the bumper thickness for a Whipple shield should be 20% of the diameter of the largest impacting particle the shield is to be designed to stop at 7 km/s, normal impact angle. Another ratio to consider is given below:
$$t_b/(S^{1/2}\, t_w{}^{1/2}) = 0.07 \pm 0.02$$
Bumper thickness should be maintained within this range or the shield will be nonoptimized. On bumper materials, the best projectile breakup is obtained with bumper material density approximately the same as the projectile (i.e., "like on like"). Porous or mesh bumpers (30% to 50% voids) followed by a continuous bumper layer produce superior projectile breakup and debris cloud dispersion.
3. Enhanced shielding materials. NASA has found that against an orbital debris threat consisting mainly of aluminum particles, ceramic fabric materials (such as Nextel^{TM}) in

the outer bumper(s) produce excellent projectile breakup without contributing damaging bumper fragments to the debris cloud. Kevlar™ or other high-strength ballistic protection type fabric lower in the shield, or as the rear wall of the shield, will slow debris cloud expansion and defeat fragments in the debris cloud.

4. Multiple bumper layers. Two to four bumper layers will provide superior protection to a single bumper. Figure 12 illustrates BLEs at normal impact for equal mass Whipple and Flexible Multishock shield (assumes a 22cm standoff). At 6.5 km/s, normal impact, the MS shield stops a 40% larger projectile.
5. Rear wall properties matched to shield type. Whipple shields with low standoff (S/d < 20) will be subject to spall failure of the rear wall. To reduce spall, rear walls with spall liners, honeycombs, laminated layers, high tensile strength materials (i.e., carbon composites) all have potential to reduce weight/increase performance. Rear walls of high-standoff Whipple shields (S/d > 30) will be subject primarily to fragment failure from high-velocity, point particle loads. Materials that are more effective at reducing high-velocity penetration on an equal weight basis will increase performance (ceramics, graphite-epoxy, etc.). Rear walls of multiple bumper shields (e.g. MS shields) will be subject to impulsive loads and bending forces from lower velocity debris clouds (usually impacting at small fraction of impact velocity). High-strength and high-strain to failure materials (such as Kevlar™) offer weight reduction potential for rear walls of the multi-bumper, MS type of shield.

CONCLUDING REMARKS

Semi-empirical ballistic limit equations have been developed for ISS shields based on HVI data. Whipple shields are generally less effective than multiple layer shields for M/OD protection. On ISS, Whipple shields are used in areas less exposed to M/OD impact (aft and Earth-facing directions). In areas exposed to a higher flux of M/OD impacts (ram and port/starboard side directions), multilayer shields containing Nextel™ ceramic fabric and Kevlar™ high-strength fabric are often used on ISS to reduce weight and increase shielding performance.

Acknowledgment—The authors thank Boeing personnel including Russell Graves, Darrell Winfield, and David Williams, and the ISS Structures Manager/JSC Kornel Nagy, for contributing Node and Common Module targets for hypervelocity impact testing. In addition, the authors appreciate the assistance from NASA HVI test personnel Jeanne Crews/JSC, Mike Kirsch/WSTF, Chuck Cornelison/ARC, as well as Lockheed and G.B. Tech personnel Dana Lear, Tom Prior, Frankel Lyons, Freeman Bertrand, Jay Laughman, Ron Bernhard, Jim Hyde, Bill Davidson, Adam Andrea, and Bobbie Simpson.

REFERENCES

[1] Zolensky ME, Zook HA, Horz F, Atkinson DR, Coombs CR, Watts AJ *et al.*, Interim Report of Meteoroid and Debris Special Investigation Group, *LDEF 69 Months in Space – 2nd Post-Retrieval Symposium,* NASA CP-3194, 277-302 (1993).

[2] Christiansen EL, Design Practices for Spacecraft Meteoroid/Debris (M/D) Protection," Hypervelocity Shielding Workshop Proceedings, Institute of Advanced Technology Catalog Number IAT.MG-0004 (1999).

[3] NASA Johnson Space Center (JSC) Hypervelocity Impact Technology Facility (HITF) web page, location (URL) http://hitf.jsc.nasa.gov/hitfpub/main/index.html

[4] NASA JSC White Sands Test Facility web page, http://wstf.nasa.gov

[5] Cour-Palais BG, Meteoroid Protection by Multi-Wall Structures, AIAA Hypervelocity Impact Conference, AIAA Paper No. 69-372 (1969).

[6] Cour-Palais BG and Crews JL, A Multi-Shock Concept for Spacecraft Shielding, *Int. J. Impact Engng*, **10**, pp.135-146 (1990).

[7] Cour-Palais BG, A Career in Applied Physics : Apollo through Space Station, *Int. J. Impact Engng,* **23,** pp.137-168 (1999).
[8] Christiansen EL, Design and Performance Equations for Advanced Meteoroid and Debris Shields, *Int. J. Impact Engng,* **14,** pp.145-156 (1993).
[9] Cour-Palais BG and Dahl K, Standardization of Impact Damage Classification and Measurements for Metallic Targets, NASA Johnson Space Center (1990).
[10] Christiansen EL, Crews JL, Williamsen JE, Robinson JH, Nolen AM, Enhanced Meteoroid and Orbital Debris Shielding, *Int. J. Impact Engng,* **17,** pp. 217-228, 1995.
[11] Christiansen EL and Kerr JH, "Mesh Double-Bumper Shield: A Low-Weight Alternative for Spacecraft Meteoroid and Orbital Debris Protection," *Int. J. Impact Engng,* **14,** pp. 169-180, 1993.
[12] Christiansen EL, Kerr JH, De La Fuente HM, Schneider WC, "Flexible and Deployable Meteoroid/Debris Shielding for Spacecraft," *Int. J. Impact Engng,* **23**, pp.125-136, 1999.